Sensors and Materials, Vol. 33, No. 9 (2021) 3269–3282
MYU Tokyo

S & M 2687

Three-dimensional Printing of Product Design Models Using Continuous-fiber-reinforced Composites

Cheng Cheng*

College of Fine Arts, Chongqing Three Gorges University, Wanzhou 400065, China

(Received March 23, 2021; accepted July 16, 2021)

Keywords: 3D printing technology, process optimization, fused deposition modeling technology, product design modeling, continuous-fiber-reinforced composites

Three-dimensional (3D) printing has the main advantages of a high material utilization rate, diversified design, rapid prototyping, the ability to form complex products, high printing speed, and high quality of printed products. Fused deposition modeling (FDM) technology can rapidly generate models with different structural characteristics and then transform the models into actual products. In this study, considering the basic principles of FDM, we first analyzed the process flow and the factors affecting 3D printing. The principle of separating the model and adding support was discussed. Next, the types of support of the model were classified. Finally, the process integrity of different models was studied using examples, and an optimal design scheme for different types of support was proposed. The rapid development of 3D printing technology is expected to realize the effective manufacturing of composite structures with complex geometric shapes, thus further expanding the application range of composite materials. Therefore, in this study, from the perspective of mechanical properties, we analyzed the research status of 3D printing using continuous-fiber-reinforced composites (CFRCs) and performed tests in terms of bending properties. The results show that, on the one hand, adding different types of support can improve the forming process and quality of the products. On the other hand, the effects of bending properties on the mechanical properties and damage evolution law of 3D-printed CFRC products were obtained under typical loads, and a strength/stiffness analysis and a prediction method were used to determine the main factors that affected the mechanical properties.

1. Introduction

Three-dimensional (3D) printing is a printing technique, and a 3D printer (3DP) is a type of manufacturing equipment based on rapid prototyping technology that integrates new materials, digital information, artificial intelligence, and other technical features.(1) Since its birth in the 1980s, 3D printing technology has developed rapidly and is now used in a wide range of fields such as architectural model design, medical equipment production, and the production of aerospace and spacecraft parts.(2) 3D printing has three main advantages over conventional

*Corresponding author: e-mail: jydkbjb@126.com
https://doi.org/10.18494/SAM.2021.3385

ISSN 0914-4935
https://myukk.org/

processing methods. First, the 3D printing technology transforms 3D solid processing into discrete stacking processes to form products. Second, the 3D printing model reduces the complexity of manufacturing. Third, the 3D printing model enables data to be imported directly and accurately by the machining equipment, resulting in the rapid generation of 3D products and the processing and manufacturing of complex parts.(3)

3D printing technology started relatively late in China, but China is now a world leader in some fields of 3D printing technology. For example, Shared Equipment Co., Ltd. launched an industrial-grade casting 3DP in 2015 whose processes, materials, software, integration, and equipment were all developed in China. In 2018, research projects were undertaken by Huazhong University of Science and Technology and other organizations to increase the worldwide competitiveness of China's additive manufacturing and casting field. Moreover, domestic universities have made great progress in laser rapid prototyping systems, laser melt deposition methods, electron beam selective melting, and other technologies.

3D printing has a wide range of applications in many fields and many advantages, such as material saving and diverse uses in manufacturing. However, the limited range of materials suitable for 3D printing poses challenges in the utilization of materials, so it is necessary to develop a wider range of materials suitable for 3D printing.(4) Owing to 3D printing, if there is a 3D model of an object, it can be copied and printed indefinitely. The intellectual property of 3D printing is an urgent problem that must be solved.(5) 3D printing has a diverse range of uses (e.g., there are already reproductions of organs printed from data of living organs, raising ethical questions).(6) Currently, industrial-grade 3DPs are expensive, often costing tens of millions of dollars. If 3DPs are to enter widespread use, their prices must be lowered.

3D printing technology simplifies the traditional processing technology of parts, greatly reduces the production cycle, and is suitable for efficient and distributed processing. 3DPs using fused deposition modeling (FDM) technology have advantages of a simple mechanical structure, convenient equipment operation, and low material cost.(7) In this paper, on the basis of 3D printing using FDM technology, we analyze the entire process from modeling to post-processing, summarize methods that improve the processing performance, and suggest ways to improve the manufacturing process of parts. Also, the mechanical behavior and damage rule of 3D-printed continuous-fiber-reinforced composites (CFRCs) under bending deformation are discussed, and a method of analyzing the strength/stiffness of CFRCs is introduced.

2. Related Works

3D printing technology has been developing rapidly in recent years. After restructuring and integration, the international leaders in the field are 3D Systems, Stratasys, and Shapeways from the US and RepRap from the UK.(8) In 2019, 3D Systems launched ten new materials for the 2S-HT90 3DP. These materials can be used for durable goods and automotive applications because of their robustness in high-temperature environments. Moreover, the biocompatibility of these materials makes them suitable for healthcare applications. Stratasys made headway in the FDM process at the beginning of 2020 and developed the F370 printer, whose user-friendly design improved the degree of automation of the equipment.

At present, the main processes of 3D printing are FDM,(9) selective laser sintering or melting (SLS/SLM),(10) stereolithography,(11) direct energy deposition,(12) and layered solid manufacturing.(13) FDM involves melting a filamentous hot melted material and extruding the material using an extruder with a micronozzle. In accordance with the imported model, the nozzle moves along the X and Y directions to form the top layer of the model. After the upper layer of the model is completed, the worktable descends by a distance equal to the thickness of one layer in the Z direction in accordance with the predetermined displacement, then the next layer is formed. Such layer-by-layer formation is repeated until the entire model has been completed. The operation principle of a 3D printing machine is shown in Fig. 1. The common methods of 3D printing have different applications in different fields depending on their process characteristics. However, these processes are all based on the principle of dispersion/accumulation to process parts from scratch.(14)

In theory, 3D printing technology can achieve absolute accuracy. However, to obtain higher precision in practical production, it is necessary to study the technology and the problems of control, e.g., size accuracy, shape accuracy, and surface accuracy. Many factors affect the accuracy of rapid prototyping, particularly the preprocessing, forming processing, and post-processing errors.(15) Moreover, the manufacturing characteristics of 3D printing technology also make products prone to internal defects. Therefore, the composition distribution and solidification microstructure characteristics, the formation mechanism and control method of internal defects in components, and the action mechanism and detection method of internal defects and their effects on the performance of components are also important research directions. Furthermore, 3D printing technology cannot be widely used in China because of the high cost of the equipment.

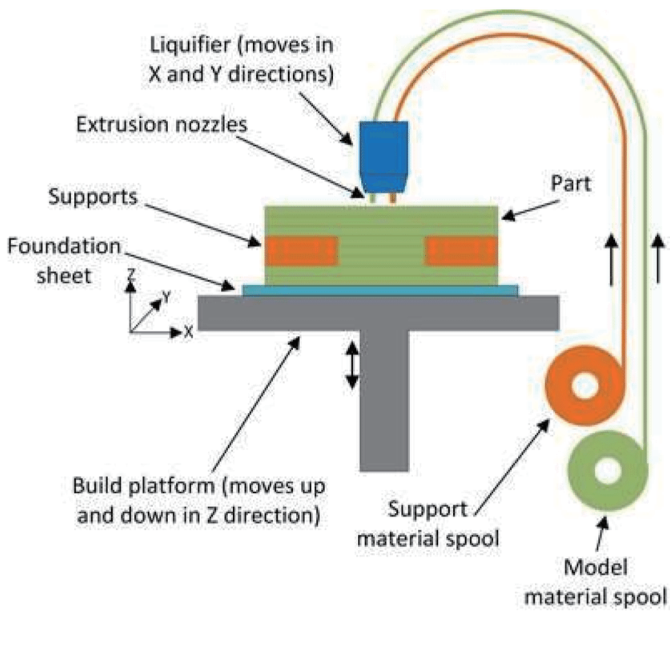

Fig. 1. (Color online) 3D printing machine using FDM.

3. Product Design Modeling of 3D Printing and Factors Affecting It

3.1 Product design modeling of 3D printing

3D printing can be used for a wide variety of materials, from plastics to metals, ceramics and rubber, and even food. The general process of 3D printing includes five parts: 3D modeling, 3D digital slicing, 3DP loading, layered processing, and superimposed molding.[16] Firstly, SolidWorks software is used for 3D modeling in accordance with the 3D printing process. Meanwhile, the model structure and process are optimized. Then Cura software is used to process the data and set the 3D printing process parameters. Finally, 3D printing and post-processing are carried out to realize the printed object. The printing process is shown in Fig. 2. Rhino modeling software can be used to complete the 3D model. Then, Magic software is used to determine the data cutting layer, and the model is saved as a *.stl file that is imported by the 3DP. After setting the support position and section filling type required by the model, the printed object can be self-layered.

3.2 Effects of 3D printing parameters on modeling product design

(a) **Temperature**: Printing and platform temperatures refer to the temperature to which the nozzle of the 3D printing equipment heats the filamentous material and the operating temperature of the bearing platform, respectively. The temperature of the nozzle determines the viscosity and fluidity of the extruded filamentous material. The platform temperature affects the adhesiveness and thermal shrinkage of the molded parts.

(b) **Fill**: Filling degree refers to the percentage of filling material inside the model relative to the total model volume. In machining, the material at the boundary part of the model will spill out to the outside if the filling degree is very high, which will reduce the dimensional accuracy of the parts, for example, the actual size of an inner hole may be smaller than the theoretical size, and the actual size of an outer circle may be larger than the theoretical size.

Fig. 2. (Color online) 3D printing process.

(c) **Thickness**: Layer thickness refers to the thickness of the slice layer. Each layer of the slice is equivalent to approximating an oblique column with a straight column. The thicker the layer is, the greater the error of the approximate substitution will be, resulting in a low degree of surface reduction and a low processing accuracy of the final model.
(d) **Printing speed**: Printing speed refers to the speed at which the nozzle of the machine moves. If the printing speed is very high, staggered layers are more likely to be formed. However, a very low printing speed will prolong the printing time and reduce efficiency. Therefore, it is necessary to set a suitable printing speed that ensures both the efficiency and the precision of processing.
(e) **Placement posture of the model**: If the initial position of the model is unreasonable, the modeling against the gravitational process may occur, resulting in the instability of the model under stress in the processing process and seriously affecting the integrity of the process.
(f) **Dimensions of molded parts**: Models within the allowable processing size range of the printer equipment are regarded as models of a permitted size. If the forming part is very large, it must be split into models of a permitted size. If the forming part is very small, the contact surface between the model and the bearing platform will be small. It is easy for a model to become unstable during processing, so it is necessary to increase the auxiliary process support.
(g) **Nozzle diameter**: Nozzle diameter is the diameter of the discharge hole of the heated head of the 3DP. The nozzle diameter is an inherent parameter of the 3DP and determines the diameter of the filamentous material emitted by the 3DP.

4. 3D Printing Process Optimization Design

When printing a 3D model, the size of the molded parts should be within the size range allowed for printing (including the length, width, and height). If the molded part is very large, it is split into several sub-blocks conforming to the permitted size of the molded parts for the printer. For molded parts that do not need to be split, we consider the type of support that the molded part requires. The types of support are unbraced support, automatic support, and manual support. During the slicing process by slicing software, the placement posture and support position of the molded parts should be considered.(17)

4.1 General principles for model splitting

Molded parts whose size exceeds the allowable working space of the 3DP must be split into sub-blocks, and then the split parts are spliced together to assemble the required molded parts.(18)

4.1.1 Control the number of sub-blocks

By considering the working range of the 3DP, the number of sub-blocks into which the layout of the molded part should be split is determined. The number of sub-blocks should be as small as possible because the assembly of sub-blocks will reduce the precision and increase the subsequent work required for assembly.

4.1.2 Add location and connection structures

To improve the stitching accuracy and strength of the sub-blocks, a positioning structure, such as a boss and groove, can be designed to match the connection in accordance with the stitching mode (e.g., screw hole and buckle) and stitching position of the molded parts.

4.1.3 Layout of molded parts

The size, shape, type of support, splitting position, and machining direction of the sub-blocks affect the precision and stitching of the molded parts. To ensure the forming accuracy and the integrity of the processing technology, the size of each sub-block should be similar, the direction of the stitching surface should be the same for all sub-blocks, and contact between the stitching surface and the auxiliary support should be avoided.

4.1.4 Examples of application

Figure 3 shows the design and modeling of a sample product with a size of 300 mm × 300 mm. The maximum processing size of the selected 3DP is 170 mm × 170 mm. The split lines are set at the positions of the horizontal and vertical symmetry centerlines so that the sizes of the four sub-blocks are similar, and the structures of screw holes and stiffeners are added inside the molded parts to ensure the stitching accuracy and strength while preserving the aesthetics of the molded parts as much as possible. Figure 3 shows the sub-blocks and their auxiliary support structure. The size of each sub-block is about 150 mm × 150 mm. We can select the upper part of the bottom surface as the datum for processing.

4.2 Unsplit model

If the dimensions of the molded parts are all within the size range limit of 3DP processing, the type of support should be selected. The types of support are manual support, automatic support, and unbraced support.

Fig. 3. (Color online) Sub-blocks and auxiliary support structure in 3D printing.

4.2.1 Unsupported product design modeling

The unsupported molded parts can be printed if the appropriate printing datum is selected to be in contact with the bearing platform. The molded parts are smaller at the top and larger at the bottom, i.e., the entire model is conical, and the chassis is relatively large. For example, the designed molded part is a hollow cylinder with a diameter and height of 50 mm and a wall thickness of 5 mm, so there is no need for segmentation. The molded parts are stable without the need to add manual support, and there is no hanging part. Table 1 shows key parameters of Cura slicing software. In Fig. 3, black represents the surface of the molded parts, and gray represents the section of a certain layer of the molded parts. The consumables and processing time of the model are also calculated and displayed by the software. Compared with the molded parts that need a support, this type of molded part has a relatively simple structure and is easy to process and shape.

4.2.2 Product design modeling of automatic support

When the molded part has a suspended structure, a supporting structure should be set below the suspended part before slicing, and the supporting structure should be printed together with the product during forming. There are two types of automatic support with supporting materials in Cura slicing software. One is Everywhere, which means that the bottom of all suspended parts on the molded parts will be supported. The other is a touching BuildPlate, i.e., the support is only added to the bottom of the overhanging part where the printing platform is. A floating molded part at the bottom is usually supported by a touching BuildPlate, and the bottom surface is selected as the base for printing. In the state diagram of layers 1 to 85 obtained by Cura slicing software, the middle section is the molded part and the gray section denotes the linear automatic support. The surface in contact with the support is very rough and does not meet the precise requirements of the contact fit of the molded parts. Therefore, it is necessary to avoid contact between the support and the high-precision molding surface.

4.2.3 Product design modeling of manual support

Manual support means that support is directly added to the position where it is needed in the 3D model design to ensure the stability of the molded part during the machining process and the integrity of the process. For a small molded part having a small contact area with the working platform, poor self-stability, and low resistance to deformation, a manual support should be added. The following principles should be considered when setting a manual support. (1) The

Table 1
Key parameters of Cura slicing software.

Thickness	Wall thickness	Open at back	Thickness of bottom/top layers	Packed density	Printing speed	File type
0.2 mm	0.8 mm	Yes	0.75 mm	18%	30.0 mm/s	0

manual support should have sufficient stability, and the auxiliary support should not only have self-stability but also increase the stability of the molded part. (2) The manual support should be easy to remove, the contact surface between the manual support and the molded part should be as small as possible, and a thin-walled structure with a guiding function should be added between the support and the model to minimize damage to the surface of the molded part. (3) Active support should be provided by a thin-walled structure. The thin-walled supporting structure is easily formed by the nozzle in a single process, which not only saves processing time and materials but also improves printing efficiency. Figure 4 shows the force diagram of the workpiece to be processed. The molded part comprises a cylinder (10 mm diameter, 5 mm height) and a cuboid (15 mm height). Under the premise of ensuring the size and shape requirements of the molded parts, the bottom surface of the cuboid can be selected as the datum for printing.

The material melted by heating at the bottom of the molded part adheres to the platform, so there is an upward supporting force and a downward adhesive force between the molded part and the platform. The force exerted by the platform on the molded part can be simplified as the supporting force F_1 (vertically upward) and the adhesion force F_2 (vertically downward) on the left and right sides, respectively, G defines the model's gravitational mass, and F represents the horizontal thrust of the nozzle. In the processing by the 3DP, the horizontal force of the nozzle on the molded part is restricted by many factors and difficult to measure accurately. The height and width (or length) of the molded part are denoted as h and b, respectively. The nozzle moves from left to right, with the molded part being the most prone to toppling at the far-right end. The adhesion force F_2 of the molded part applied to the platform should be less than the maximum adhesion force $F_2^{\max}$ between the material and the platform at the processing temperature, while the supporting force F_1 should be less than the maximum extrusion force $F_1^{\max}$ of the forming material at the processing temperature to ensure that the molded part does not separate from the platform and to maintain its stability. According to the analysis in Fig. 4, the smaller the forces F_1 and F_2 exerted by the platform on the molded part, the higher the stability of the molded part in the machining process. From the static formulas

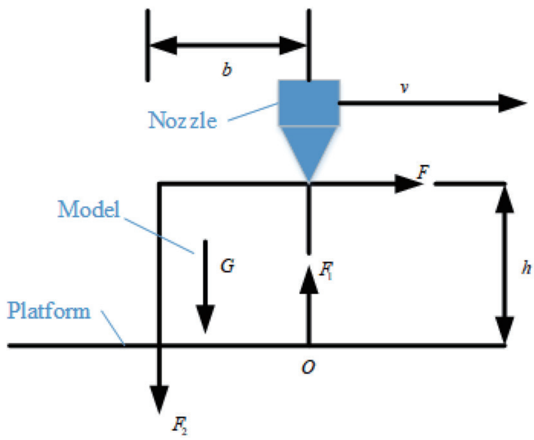

Fig. 4. (Color online) Force analysis of product design modeling.

$$G = F_1 - F_2\,, \tag{1}$$

$$F \cdot h = F_2 \cdot b + G \cdot b/2\,, \tag{2}$$

$$F_1 + F_2 = 2F \cdot h/b\,, \tag{3}$$

it can be seen that the horizontal force of the nozzle on the molded part is unchanged, and reducing the aspect ratio of the molded part (i.e., h/b) is conducive to improving its stability.

Figure 5(a) shows the design of a small molded part, where h_1 is the height of the molded part, b_1 is the length and width of the molded part, and h_1/b_1 is the theoretical critical value of the aspect ratio. The experimentally printed molded part is shown in Fig. 5(b), and the molded part is completely deformed. In the processing, the nozzle temperature is high and the aspect ratio of the molded part is greater than the critical value at a certain temperature. The heat concentration of the printing layer leads to the remelting of the printed lower layer material and the instability of the model in the processing, which eventually leads to the thermal deformation of the model. Since the aspect ratio is greater than the critical value at a certain temperature, this will lead to model processing failure. When designing the model, once the height has been determined, the aspect ratio of the model is reduced by appropriately increasing the width of the model. Figure 5(c) shows the model after manually adding a thin-wall support, taking a square support as an example: The height of the model remains unchanged, the width of the model increases from b_1 to b_2 (3.08 mm), and the aspect ratio of the model decreases from 2.0 to 0.65. Figure 5(d) shows the processed molded part after adding the thin-wall support, and Fig. 5(e) shows the actual object after removing the support. The comparative testing of the models in Figs. 5(b) and 5(e) shows that increasing the width of the model by manually adding the thin-wall support not

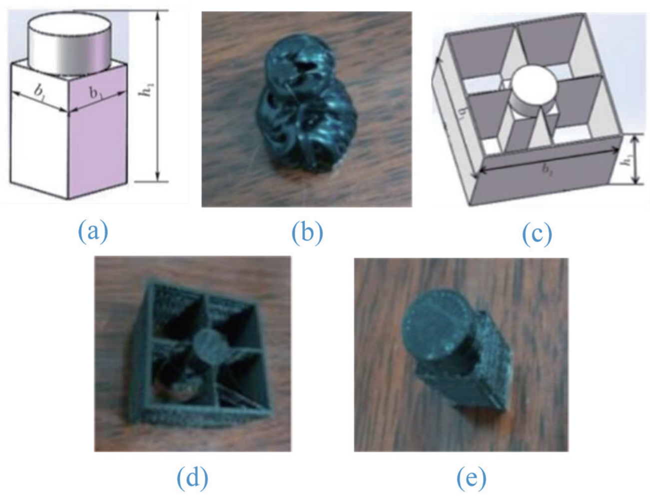

Fig. 5. (Color online) Molded parts. (a) Design of small molded part. (b) Directly processed physical object. (c) Model required in the process. (d) Added support of the physical object. (e) Object with the supporting structure removed.

only prevents the model from being unstable when the 3DP adds the next layer, which improves the stability of the model in the processing, but also reduces the intensity of nozzle heating, giving the processing materials sufficient time to cool down. This is an effective means of ensuring the machining stability and process integrity of a small model with a large aspect ratio.

5. Analysis of Bending Properties of CFRCs Using Mixing Rule

The finite element method, volume average stiffness (VAS), classical laminated plate theory, and the mixture rule of composites are usually used to analyze and study the mechanical properties and damage mechanism of 3D-printed CFRCs. In particular, the mixture law is widely used in the prediction and evaluation of the mechanical properties of composite materials. By this method, the properties of composite materials are linearly correlated with the volume content of component materials as

$$E_{11} = V_f \cdot E_f + (1 - V_f) \cdot E_m , \tag{4}$$

where E_{11} denotes the elastic modulus of the composite material in direction 1, V_f represents the fiber volume content, E_f describes the elastic modulus corresponding to the fibers, and E_m is the elastic modulus of the matrix.

When the fiber volume content is low (<11%), the mixing rule can be used to better predict the tensile properties of composites. However, when the fiber volume content is high, the prediction accuracy of the mixing method will decrease significantly. Note that in the 3D printing process, with an increase in fiber volume content, the full impregnation of the fibers will become more difficult. In addition, the void defects in 3D printing composites also increases significantly with the fiber volume fraction. This will degrade the mechanical properties of composites, resulting in a large discrepancy between the theoretical prediction results and the test results. 3D-printed composite structures can usually be divided into different regions, and the stiffness characteristics of these regions will have a significant impact on the overall stiffness of the entire structure. The VAS method is based on the hypothesis of strain continuity,[19] and the overall stiffness $[K_{ave}]$ corresponding to the entire composite structure can be theoretically deduced from the local stiffness and volume percentage corresponding to different regions in the structure:

$$[K_{ave}] = \sum_{i=1}^{n} V_i \cdot [K_i] , \tag{5}$$

where V_i is the volume percentage of part i in the 3D-printed composite material structure and $[K_i]$ is the stiffness of part i in the 3D-printed composite structure in the global coordinate system. The VAS method is adopted to analyze and predict the overall stiffness of 3D printing composite materials, which mainly includes the following three steps.[20]

(1) The effective stiffnesses corresponding to the different micromechanical molded parts of the 3D-printed composite structure are determined.
(2) The effective stiffnesses corresponding to different parts of the 3D-printed composite structure in the local coordinate system are converted to the corresponding stiffnesses in the global coordinate system by the coordinate transformation method.
(3) The volume average of the stiffnesses corresponding to different parts of the 3D-printed composite structure is determined.

6. Results and Discussion

Bending properties, as important mechanical properties of composite materials, are of great significance in the design of engineering structures. Researchers at home and abroad have conducted many experimental studies on the bending properties of 3D-printed CFRCs and have revealed the main factors affecting the bending properties of 3D-printed composites. The damage evolution law of 3D-printed composites under a bending load has also been explored.

Figure 6 shows a summary of the bending properties of 3D-printed composites in the relevant literature. The bending properties of 3D-printed composites increase significantly with increasing fiber volume content. When the fiber volume content reaches 40–50%, the bending strength of the 3D-printed composite material exceeds 500 MPa, which is the bending performance necessary for an aluminum alloy material used in aviation. The flexural strength and modulus of continuous thermosetting CFRCs prepared by 3D printing are 858.05 MPa and 71.95 GPa, respectively. Under different printing conditions, the flexural strength and modulus of continuous nylon CFRCs prepared by 3D printing reached maximum values of 565.8 MPa and 70.6 GPa, respectively.

Figure 7 shows the bending properties of 3D-printed nylon composites[21–26] for different reinforcement fibers. With the same fiber volume content, the bending properties of 3D-printed CFRCs are significantly superior to those of glass fiber-reinforced composites and aramid fiber-

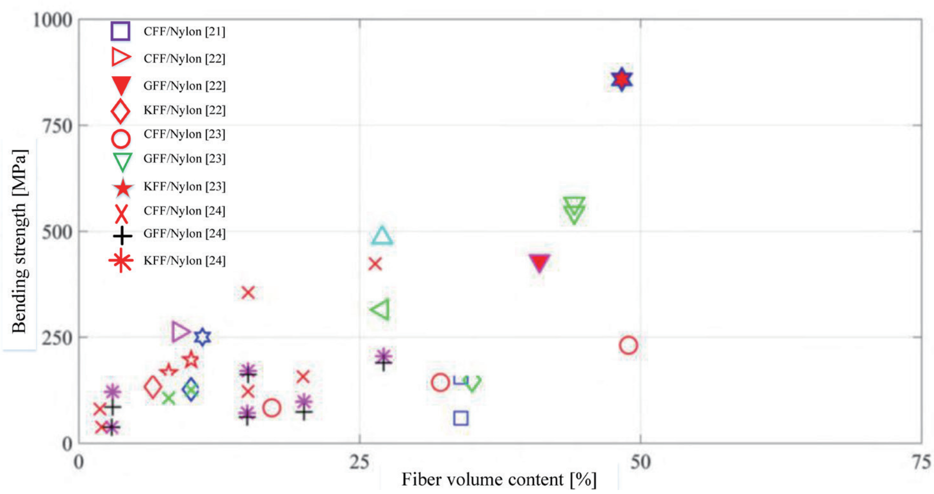

Fig. 6. (Color online) Bending properties of 3D-printed composites.

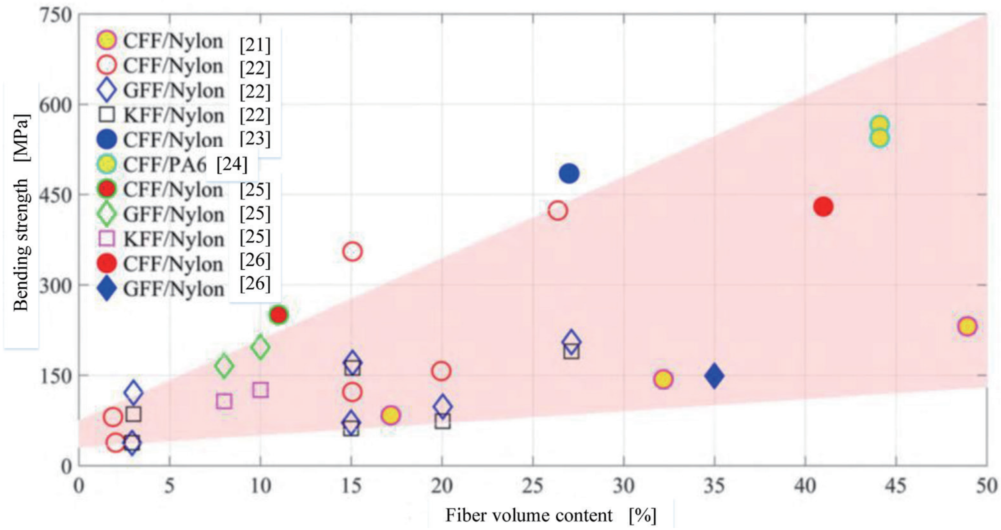

Fig. 7. (Color online) Flexural strengths of 3D-printed composites with different reinforcing fibers.

reinforced composites, and this fiber property difference is the main reason for the significant bending property difference of the composites. Damage mechanism analysis shows that marked fiber pull-out occurred in the failed section of 3D printing composites. Compared with the surfaces of carbon and glass fibers, the surface of an aramid fiber is very smooth, and there is no residual substrate material attached to it, which indicates that the interface property between the aramid fiber and the nylon matrix is weak, and fiber pull-out failure easily occurs; this is also one of the reasons for the poor bending property of aramid fiber-reinforced composites. Under the action of a bending load, the stress of composites is complex, and the fiber, fiber/matrix interface, and interface properties with an adjacent printing wire and lamination affect the bending strength of composites. In the study, it was found that the interface property difference leads to significant differences in mechanical properties and damage laws of 3D-printed composites under bending loads. When the interfacial bonding property is weak, the flexural strength of the composite is low (only 132 MPa), and a large incidence of fiber pull-out and significant lamination extensions are observed in the failure section. When the interfacial bonding performance is high, the flexural strength of the composite material significantly increases to 176 MPa and fiber failure mainly occurs in the flexural section.

7. Conclusions

Product design modeling is a creative process, that is, an individual or group activity with innovative characteristics. 3D printing technology improves design innovation in every link of the design chain. According to the FDM principle and 3D printing product design and modeling process, the processing of large and complex models was realized by optimizing the model splitting and splicing processes to improve the product quality and processing technology. For models without segmentation, automatic or manual support is added in the printing process to improve the printing quality and the molding accuracy of the model. Compared with the composites prepared by conventional technologies, the mechanical properties of 3D printing composites are still unsatisfactory. To further improve the mechanical properties, it is necessary to carry out a more in-depth study on the effects of printing process parameters, reveal the multiparameter coupling mechanism in the molding process, and lay a foundation for realizing the optimization of printing parameters.

Acknowledgments

This work was supported by the "Research on the Design of Interactive Picture Books during New Media Technology Time" Social Science Project of Chongqing University of Posts and Telecommunications.

References

1 M. Attaran: Prog. Bus. Horiz. **60** (2017) 6777. https://doi.org/10.1016/j.bushor.2017.05.011
2 A. Mostafaei, A. M. Elliott, J. E. Barnes, F. Li, W. Tan, C. L. Cramer, P. Nandwana, and M. Chmielus: Prog. Mater. Sci. **119** (2021) 100707. https://doi.org/10.1016/j.pmatsci.2020.100707
3 A. McCormack, C. B. Highley, N. R. Leslie, and F. P. W. Melchels: Trends Biotechnol. **38** (2020) 584. https://doi.org/10.1016/j.tibtech.2019.12.020
4 K. Piironen, M. Haapala, V. Talman, P. Järvinen, and T. Sikanen: Lab. Chip **20** (2020) 2372. https://doi.org/10.1039/D0LC00114G
5 D. Mahr and S. Dickel: J. Intel. Property Law Practice **15** (2020) 711. https://doi.org/10.1093/jiplp/jpaa124
6 M. Javaid and A. Haleem: Clin. Epidemiol. Global Health **8** (2020) 586. https://doi.org/10.1016/j.cegh.2019.12.008
7 S. Wickramasinghe, T. Do, and P. Tran: Polymers **12** (2020) 1529. https://doi.org/10.3390/polym12071529
8 C. T. Do, J. H. Choi, Y. S. Lee, C. H. Kim, and S. W. Chung: IEEE Embedded Syst. Lett. **13** (2021) 57. https://doi.org/10.1109/LES.2020.3001954
9 K. Gnanasekaran, T. Heijmans, S. V. Bennekom, H. Woldhuis, S. Wijnia, G. D. With, and H. Friedrich: Appl. Mater. Today. **9** (2017) 21. https://doi.org/10.1016/j.apmt.2017.04.003
10 S. L. Sing, W. Y. Yeong, F. E. Wiria, B. Y. Tay, Z. Q. Zhao, L. Zhao, Z. L. Tian, and S. F. Yang: Rapid Prototyping J. **23** (2017) 611. https://doi.org/10.1108/RPJ-11-2015-0178
11 N. Bhattacharjee, C. P. Cabrera, Y. T. Kim, A. P. Kuo, and A. Folch: Adv. Mater. **30** (2018) 180001. https://doi.org/10.1002/adma.201800001
12 Z. Liu, H. C. Zhang, S. Peng, H. Kim, D. Du, and W. Cong: Addit. Manuf. **30** (2019) 100848. https://doi.org/10.1016/j.addma.2019.100848
13 S. P. Regalla, S. S. Karwa, S. Rajesh, P. V. Shyam, and P. N. Shrivastava: Mater. Today: Proc. **28** (2020) 1030. https://doi.org/10.1016/j.matpr.2019.12.347
14 B. Smith and P. Dasgupta: World J. Urology **38** (2020) 2385. https://doi.org/10.1007/s00345-019-02995-1
15 N. K. Mauryaab, V. Rastogi, and P. Singh: CIRP J. Manuf. Sci. Technol. **29** (2020) 53. https://doi.org/10.1016/j.cirpj.2020.02.003
16 M. M. Prabhakar, A. K. Saravanan, A. H. Lenin, I. J. leno, K. Mayandi, and P. S. Ramalingam: Mater. Today: Proc. **45** (2021) 6108. https://doi.org/10.1016/j.matpr.2020.10.225
17 T. Feuerbach, S. Kock, and M. Thommes: Pharm. Dev. Technol. **25** (2020) 650. https://doi.org/10.1080/10837450.2020.1727921
18 C. Li, D. Cabrera, F. Sancho, R. V. Sanchez, M. Cerrada, and J. V. Oliveira: IEEE Trans. Ind. Electron. **68** (2021) 8768. https://doi.org/10.1109/TIE.2020.3013546
19 S. Kumar and P. Jana: Int. J. Mech. Sci. **163** (2019) 105105. https://doi.org/10.1016/j.ijmecsci.2019.105105
20 I. A. R. Marquez and V. Bolborici: Ultrasonics **77** (2017) 69. https://doi.org/10.1016/j.ultras.2017.01.019
21 M. A. Calvo, I. L. Gómez, N. C. Simon, J. L. L. Salazar, T. G. Girón, J. S. C. Cordero, and O. S. Brenes: Addit. Manuf. **22** (2018) 157. https://doi.org/10.1016/j.addma.2018.05.007
22 J. M. Chacon, M. A. Caminero, P. J. Nunez, E. G. Plaza, I. G. Moreno, and J. M. Reverte: Compos. Sci. Technol. **181** (2019) 107688. https://doi.org/10.1016/j.compscitech.2019.107688

23 L. G. Blok, M. L. Longana, H. Yu, and B. K. S. Woods: Addit. Manuf. **22** (2018) 176. https://doi.org/10.1016/j.addma.2018.04.039

24 T. Liu, X. Tian, M. Zhang, A. Dilmurat, D. Li, and Z. Gerhard: Composites Part A **114** (2018) 368. https://doi.org/10.1016/j.compositesa.2018.09.001

25 A. N. Dickson, J. N. Barry, K. A. Mcdonnell, and D. P. Dowling: Addit. Manuf. **16** (2017) 145. https://doi.org/10.1016/j.addma.2017.06.004

26 G. D. Goh, V. Dikshit, A. P. Nagalingam, G. L. Goh, S. Agarwala, S. L. Sing, J. Wei, and W. Y. Yeong: Mater. Des. **137** (2018) 79. https://doi.org/10.1016/j.matdes.2017.10.021

About the Author

Cheng Cheng received her B.S. degree from Southwest University, China, and her M.S. degree in engineering from Southwest Jiaotong University (SWJTU), China, in 2004 and 2010, respectively. In 2004, she joined the College of Fine Arts, Chongqing Three Gorges University, where she is currently a lecturer. She served as a training lecturer on the preservation of Chongqing's intangible cultural heritage, a member of Chongqing Women Painters Association, and a member of China Aesthetic Education Association in 2014, 2016, and 2019, respectively. Her research interests include 3D painting, product design modeling, and vision design. (jydkbjb@126.com)